Inorganic Chemistry
Cite This: Inorg. Chem. 2019, 58, 10871−10882
Article
pubs.acs.org/IC

# Monomeric and Trimeric Thorium Chlorides Isolated from Acidic Aqueous Solution

Jennifer N. Wacker,[†] Monica Vasiliu,[‡] Ian Colliard,[§] R. Lee Ayscue, III,[†] Sae Young Han,[†] Jeffery A. Bertke,[†] May Nyman,[§] David A. Dixon,[‡] and Karah E. Knope*[,†]

[†]Department of Chemistry, Georgetown University, 37th and O Streets NW, Washington, D.C. 20057, United States
[‡]Department of Chemistry and Biochemistry, The University of Alabama, Tuscaloosa, Alabama 35487, United States
[§]Oregon State University, Department of Chemistry, Corvallis, Oregon 97331, United States

Supporting Information

**ABSTRACT:** Two thorium(IV) compounds, $[Th(H_2O)_4Cl_4]\cdot 2(HPy\cdot Cl)$ (**1**) and $(HPy)_3[Th_3(H_2O)_2Cl_{10}(OH)_5]\cdot 4(HPy\cdot Cl)$ (**2**) (HPy = pyridinium), were isolated from acidic aqueous solution. The compounds were synthesized at room temperature and subsequently characterized using single crystal X-ray diffraction along with Raman and IR spectroscopies. Whereas compound **1** is built from discrete mononuclear $Th(H_2O)_4Cl_4$ units, compound **2** consists of a novel hydroxo-bridged trimeric $[Th_3(OH)_5]^{7+}$ core. Such species are largely absent from discussions of Th solution and solid-state chemistry and their isolation may be attributed to outer coordination sphere interactions that help stabilize the structural units; extensive hydrogen bonding and $\pi-\pi$ stacking interactions are present in **1** and **2**. Density functional theory calculations were performed to predict the respective vibrational frequencies of the structural units, and their relative stability was predicted at the correlated molecular theory level. Small-angle X-ray scattering analysis of $[Th_3(OH)_5]^{7+}$ in water indicates that the trimeric structural unit remains intact and that it is indeed an important species that necessitates consideration in geochemical models and for design of Th materials from water.

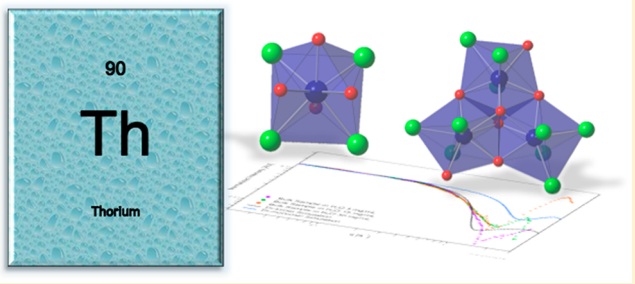


## INTRODUCTION

Metal ion speciation underpins the reactivity and toxicity along with the biological and environmental fate of metal ions.[1] Actinide (An) cations in particular can possess complex speciation profiles due to their large ionic radii, high coordination numbers, numerous accessible oxidation states, and the availability of the 5f orbitals. Fundamental knowledge of An chemistry has thus lagged behind that of main group and transition metals. Yet there is a pressing need to understand the chemical behavior of these elements as it relates to separations chemistries, waste management, and environmental mobility of actinides.[2−4] In all of these cases, discernment of the stability regime over which different An structural units persist and are stable, both in solution and the solid-state, is imperative to accurately predict the overall behavior of these radionuclides.

Factors known to govern aqueous An speciation include (1) hydrolysis and condensation, (2) ligand complexation, and (3) redox chemistry.[5] Hydrolysis and condensation reactions are pervasive to the chemistry of the tetravalent metal ions, in particular due to their high Lewis acidity, often resulting in polymeric structural units; hydrolysis and condensation products form under even very acidic conditions. The role of a coordinating ligand is less clear but complexation has led to the isolation of many unique complexes and clusters in the solid-state. Carboxylate donors have been used, for example, to thwart the progression of oligomerization, whereas in other instances such ligands have been shown to direct the assembly of larger order oligomers from smaller order polynuclear species.[6,7] Metal−ligand complexation in metal−organic frameworks has also recently been used to "trap" or otherwise direct the formation of structural units that are relatively rare in polynuclear An oxo/hydroxo structural chemistry.[8,9]

More recently, outer coordination sphere molecules and ions have likewise been shown to influence the identity of An complexes and clusters through noncovalent interactions, allowing for the stabilization and crystallization of several unprecedented monomeric and polymeric An complexes. For example, our group has shown that in U(IV) chloride systems, addition of a H-bond donor to reaction solutions that otherwise yielded $UCl_6^{2-}$ was found to result in the formation of $U(H_2O)_4Cl_4$ for which there was no literature precedence.[10] More recently, a series of thorium−nitrato complexes was reported wherein the identity of the countercation was correlated with the composition and structure of the different

Received: April 30, 2019
Published: July 29, 2019

Downloaded via OREGON STATE UNIV on June 2, 2022 at 16:19:36 (UTC).
See https://pubs.acs.org/sharingguidelines for options on how to legitimately share published articles.


© 2019 American Chemical Society

DOI: 10.1021/acs.inorgchem.9b01238
Inorg. Chem. 2019, 58, 10871−10882

Th complexes.[11] Within Np systems, Jin and colleagues demonstrated that outer coordination sphere interactions could be used to drive $Np^{V/VI}$-Cl complexation, affect the electrochemical behavior of neptunium, and thereby stabilize the higher oxidation state (VI) of neptunium.[12] Furthermore, within the broader inorganic chemistry community, strategies harnessing outer coordination sphere interactions, including ion pairing and hydrogen (H) bonding, have been used to isolate elusive metal−oxide clusters.[13−15] Noncovalent interactions have thus been shown to play an important role in species formation, stability, and precipitation; however, our understanding of the role that these interactions have on "templating" and/or stabilizing the formation of metal−ligand complexes or clusters is still in its infancy.

Of the early actinides Th−Pu, Th exclusively exists in the tetravalent oxidation state under ambient aqueous conditions, thus limiting the complication of redox chemistry in elucidating its aqueous behavior. It is the largest and least Lewis acidic of the tetravalent metal ions, yet exhibits fairly extensive hydrolysis and condensation chemistry, which has historically complicated interpretation of solution based studies and resulted in large discrepancies in thermodynamic literature.[3] Over 1000 Th solid state structures have been reported in the Cambridge Structural Database[16] and of those, approximately 50 arise from hydrolysis and condensation to include dimeric,[17−21] trimeric,[22−25] tetrameric,[26] hexameric,[27−34] octameric,[35,36] and decameric units,[37] with the hexameric $[Th_6(OH)_4O_4]^{12+}$ species being the most prevalent. Yet the $[Rn]5f^0$ electron configuration of Th has limited the number of spectroscopic handles available to assess the correlation between these solid state structural units and those present in solution, although it promotes ease when performing electronic structure calculations. As such, there remains a need to not only isolate and characterize Th hydrolysis products in the solid state but also understand the factors that govern their assembly and the conditions over which various structural units are stable.

Toward this end, we have investigated the structural chemistry of Th complexes that form in acidic aqueous solutions in the presence of noncoordinating H-bond donor molecules. Utilization of pyridinium in these systems aimed at uncovering the effects of the second coordination sphere interactions on An speciation. Herein, we report the synthesis of $[Th(H_2O)_4Cl_4]\cdot 2(HPy\cdot Cl)$ (**1**) and $(HPy)_3[Th_3(H_2O)_2Cl_{10}(OH)_5]\cdot 4(HPy\cdot Cl)$ (**2**), which are built from monomeric and trimeric Th structural units, respectively. The identities of **1** and **2** were confirmed by Raman and IR spectroscopies. Electronic structure calculations were also used to determine the relative stability of these structural units in relation to one another. The correlation between solution and solid state speciation was also examined using small-angle X-ray scattering (SAXS).

## EXPERIMENTAL PROCEDURES

**Syntheses.** ***Caution!*** *$^{232}$Th is an α emitter and standard precautions for handling radioactive materials should be followed when performing the syntheses that follow.* Thorium tetrachloride (International Bio-Analytical Industries, Inc.), pyridine (Alfa Aesar), and hydrochloric acid (Fisher Chemical) were used as received from commercial suppliers. Aqueous solutions were prepared using nanopure water (≤0.05 μS) purified by a Millipore Direct-Q 3 UV water purification system.

An aqueous solution of Th(IV) in HCl was prepared in a 3 mL glass vial by dissolving $ThCl_4$ (0.05 g, 0.13 mmol) into 1 M HCl (0.5 mL). Pyridine (20 μL, 0.25 mmol) was then added, and the solution was left to completely evaporate under a nitrogen atmosphere. After approximately 7−14 days, colorless crystals of $[Th(H_2O)_4Cl_4]\cdot 2(HPy\cdot Cl)$ (**1**) and $(HPy)_3[Th_3(H_2O)_2Cl_{10}(OH)_5]\cdot 4(HPy\cdot Cl)$ (**2**) as well as a microcrystalline powder, later identified via powder X-ray diffraction as **2**, were obtained. Crystals of **1** generally can be described as colorless blocks that possess moderate stability under ambient conditions, yet are hygroscopic and will decompose in air upon extended exposure (>30 min). Crystals of **2** are similarly colorless but adopt a prismatic morphology and are much more air-sensitive than **1**; decomposition can occur over several minutes if not kept under inert conditions or under paratone. Yield estimations, elemental analysis, and subsequent bulk analysis were complicated by the difficulty in manually separating the two phases coupled with the instability of the compounds.

**X-ray Structure Determination.** Single crystal X-ray diffraction data for **1** and **2** were collected using a Bruker Quest D8 diffractometer equipped with an IμS X-ray source using Mo Kα radiation (λ = 0.71073 Å) and a CMOS detector at 100 K. Single crystals of **1** and **2** were isolated from the bulk and mounted on MiTeGen Micromounts in mineral oil. Unit cells were identified using APEX2 and the data were integrated and filtered for statistical outliers using SAINT.[38] An absorption correction was applied to both compounds using SAINT/SADABS v2014/2.[38] Unless otherwise noted, all H atoms were placed in calculated positions and assigned as 1.2 times carrier $U_{eq}$. Crystallographic details for **1** and **2** are presented in Table 1.

**Table 1. Crystallographic Details for 1 and 2 at 100 K**

| | 1 | 2 |
|---|---|---|
| Formula | $C_{10}H_{20}Cl_6N_2O_4Th$ | $C_{35}H_{51}Cl_{14}N_7O_7Th_3$ |
| MW (g/mol) | 677.02 | 1874.24 |
| $T$ (K) | 100(2) K | 100(2) K |
| crystal system | orthorhombic | monoclinic |
| space group | *Pnma* | *C*2/*c* |
| λ (Å) | 0.71073 | 0.71073 |
| *a* (Å) | 13.7454(7) | 18.8079(8) |
| *b* (Å) | 12.1382(6) | 13.3050(5) |
| *c* (Å) | 12.2247(6) | 24.3184(10) |
| α (deg) | 90 | 90 |
| β (deg) | 90 | 108.327(1) |
| γ (deg) | 90 | 90 |
| volume (Å$^3$) | 2039.62(18) | 5776.7(4) |
| *Z* | 4 | 4 |
| ρ (g/cm$^3$) | 2.205 | 2.155 |
| μ (mm$^{-1}$) | 8.112 | 8.399 |
| R1 | 0.0297 | 0.0202 |
| wR2 | 0.0703 | 0.0375 |
| GOF | 1.391 | 1.044 |
| CCDC | 1904844 | 1904843 |

**Compound 1, $[Th(H_2O)_4Cl_4]\cdot 2(HPy\cdot Cl)$.** A structural model consisting of Th bound to two chlorides and three water molecules, one free Cl anion, one-half pyridinium cation, and one full pyridinium cation per asymmetric unit was developed. The latter pyridinium ring was disordered over a symmetry site and refined using a PART −1 command, which ignored the symmetry of the ring to allow for the proper assignment and placement of each atom in the ring. The ring was further constrained to be a perfect hexagon and restrained to behave isotropically. The anisotropic *U* values of the entire structure were restrained with rigid bond restraints. Water H atoms were located in the difference map and their corresponding distances were restrained to be 0.88 (0.02) Å. The H atom bound to the nitrogen within the nondisordered pyridinium ring was located in the difference map and restrained to a distance of 0.86 (0.02) Å. The



DOI: 10.1021/acs.inorgchem.9b01238
Inorg. Chem. 2019, 58, 10871−10882

H atom on the disordered pyridinium cation could not be found and was therefore placed in a calculated position.

**Compound 2, $(HPy)_3[Th_3(H_2O)_2Cl_{10}(OH)_5]\cdot 4(HPy\cdot Cl)$.** A structural model consisting of two-thirds of the Th trimeric unit, two free Cl anions, and three and one-half pyridinium cations per asymmetric unit was developed. Three of the pyridinium rings (rings containing N1−N3) were positionally disordered and therefore restrained to behave relatively isotropic. Rigid bond restraints were additionally applied. One of the pyridinium rings (rings containing N4) was constrained to be a perfect hexagon. The nitrogen atom (N1) on one of the pyridinium rings was constrained to have equal anisotropic displacement parameters of a nitrogen atom (N4) on another pyridinium ring. Water H atoms and hydroxide H atoms were located in the difference map. The O−H distances were restrained to be 0.88 (0.02) Å. The pyridinium N−H atoms could not be located in the difference map and thus were placed in calculated positions at 0.86 (0.02) Å.

**Powder X-ray Diffraction.** Data were collected on a Rigaku Ultima IV X-ray diffractometer (Cu K$\alpha$ radiation, $\lambda$ = 1.542 Å) at room temperature using a D/teX silicon strip detector from 3 to 40° 2$\theta$. Agreement between the calculated patterns for **1** and **2** and the experimentally observed pattern for the bulk sample (Figure S3) supported the assumption that the two phases used for structure determination were representative of the bulk sample.

**Vibrational Spectroscopy.** Infrared spectra were attained using a PerkinElmer Spectrum 2 FTIR spectrometer with an ATR-FTIR stage. Crystals of **1** and **2** were placed directly on the stage and collected over $\Delta\nu$ 400−4000 $cm^{-1}$. Raman spectra were collected on single crystals of **1** and **2** using a Horiba LabRAM HR Evolution Raman spectrometer with circularly polarized radiation and an excitation line of 532 nm. Data were collected at room temperature over $\Delta\nu$ 100−4000 $cm^{-1}$. In the Raman spectrum of **2**, the region between 1600−3000 $cm^{-1}$ does not contain any vibrations assigned to the compound. The "steps" observed in the Raman spectrum are instead a result of burning through a spot on the crystal and then moving to another area to continue data collection. Therefore, a difference in background intensity can be observed.

**Small Angle X-ray Scattering (SAXS).** The bulk sample containing crystals of **1** and **2** was dissolved in water at three concentrations (5, 15, and 30 mg/mL) to examine the stability of the complexes upon dissolution. Note: it was impossible to manually separate a phase pure sample of **2** from **1**, so we assume we start with a mixture of both trimer and monomer. However, since SAXS is a solution technique, conversion from monomer to trimer, or vice versa can be observed and tracked under different solution conditions. All solutions were filtered (Target2 NYLON, 0.45 $\mu$m) and sealed in 1.5 mm glass capillaries (Hampton Research). Data were collected on an Anton-Parr SAXSess instrument using Cu K$\alpha$ radiation ($\lambda$= 1.542 Å) and line collimation. Data were recorded over the $q$ range of 0.08−2.5 $Å^{-1}$ on an image plate detector, at a distance of 26.1 cm from the X-ray source. SAXSQUANT software was used for data collection, treatment, and preliminary analyses (normalization, primary beam removal, background subtraction, desmearing, and smoothing). Further modeling of the data was performed using the IRENA[39] macros within the IGORPro 6.3 software suite. Simulated scattering curves of the monomer in **1** and the trimer in **2** were calculated from SolX[40] using a structural file (*xyz*) derived from the SCXRD data.

**Computational Details.** The geometries were optimized at the density functional theory (DFT)[41] level with the hybrid B3LYP.[42,43] Initially, the DFT-optimized DZVP2 basis set[44] for H, O, and Cl atoms were used and then we reoptimized the structures with the aug-cc-pVDZ[45,46] basis sets for H and O, aug-cc-pV(D+d)Z for Cl,[47,48] and cc-pVDZ-PP basis sets[49] for Th using Gaussian09 program system.[50] Vibrational frequencies were calculated to show that the structures were minima. For comparison, single point CCSD(T) calculations were performed at aug-cc-pVDZ/cc-pVDZ-PP (Th) level. The single point MP2[51,52] energies were extracted from the CCSD(T) calculations. The CCSD(T) calculations utilized the MOLPRO program.[53]

Using the gas phase geometries, the solvation free energies in water at 298 K were calculated using the self-consistent reaction field (SCRF) approach[54] with the COSMO parameters[55,56] as implemented in Gaussian 03.[57] For the COSMO [B3LYP//DZVP2/aug-cc-pVDZ(-PP)] calculations in Gaussian, the radii developed by Klamt and co-workers were used to define the cavity.[55,56] The aqueous Gibbs free energy (free energy in aqueous solution), $\Delta G_{aq}$, was calculated from eq 1. The $\Delta G_{aq}$ values were corrected by 4.3 kcal/mol for each water molecule.

$$\Delta G_{aq} = \Delta G_{gas} + \Delta\Delta G_{solv} \quad (1)$$

$\Delta G_{gas}$ is the gas phase free energy and $\Delta\Delta G_{solv}$ is the aqueous solvation free energy calculated as differences between the conjugate base and the acid. A dielectric constant of 78.39 corresponding to that of bulk water was used in the COSMO calculations. The solvation energy is reported as the electrostatic energy (polarized solute−solvent).

## RESULTS

**Structure Descriptions.** Compound **1**, $[Th(H_2O)_4Cl_4]\cdot 2(HPy\cdot Cl)$, crystallizes in the *Pnma* space group. The structure is isomorphous to a previously reported U-based phase[10] and consists of Th(IV) metal centers bound to four chloride ions and four water molecules. The ligated chloride ions arrange to sit just above a plane about the Th metal center while three water molecules sit below the plane and one water molecule above the plane to form a charge-neutral structural unit. Th−$O(H_2)$ and Th−Cl bond distances range from 2.432(5) to 2.496(6) and from 2.718(1) to 2.775(2) Å, respectively. These distances are consistent with previous reports of Th−$O(H_2)$ and Th−Cl bonds, respectively.[17,27,28,58,59] The calculated DFT (B3LYP/aug-cc-pVDZ/cc-pVDZ-PP) Th−$O(H_2)$ bond distances are longer than experiment ranging from 2.52 to 2.70 Å and the Th−Cl bond distances are between 2.68 and 2.78 Å. Differences between experimental versus calculated values are typical of the B3LYP functional for these types of molecules.[10] Two pyridinium cations and two chloride anions exist in the outer coordination sphere per structural unit, linking the $Th(H_2O)_4Cl_4$ monomers together through weak to moderate H-bonding interactions.[60,61] H-bonding interactions between bound water molecules and lattice chloride ions yield O1/O3···Cl3 donor−acceptor distances ranging from 3.035(5) to 3.048(5) Å. In addition, the protonated pyridinium engages in H-bonding interactions with free chloride ions (N1-(H)···Cl1 = 3.448(6) Å) and bound water molecules (N1-(H)···$O3(H_2)$ = 2.992(10) Å). These H-bonding interactions can similarly be classified as moderate to weak.[60] Further $\pi-\pi$ stacking interactions between pyridiunium rings serve to stitch this compound together to form an extended network, illustrated in Figure 1. These interactions were calculated using Platon;[62] $C_{HPy}\cdots C_{HPy}$ = 3.613(2) and 3.644(2) Å with a slip angles of 20.0° and 18.2°, respectively.

The structure of **2**, $(HPy)_3[Th_3(H_2O)_2Cl_{10}(OH)_5]\cdot 4(HPy\cdot Cl)$, consists of a trimeric structural unit that crystallizes in the *C*2/*c* space group. Two unique Th metal centers make up the trimer (Figure 2a); Th1 is eight coordinate bound to four chlorides and four oxygen atoms. Two of the four oxygens (O1) are $\mu_2$-hydroxides while the remaining two oxygen atoms (O2) are $\mu_3$-hydroxides; the $\mu_3$-hydroxides/$\mu_2$-hydroxides bridge adjacent Th metal centers. Bond valence summation (BVS) values are consistent with hydroxide groups (Table S1). Th1−O1 and Th1−O2 distances are 2.386(1) and 2.483(2) Å, respectively. Th2 is also eight coordinate with one water molecule replacing one of the bound chlorides resulting in



DOI: 10.1021/acs.inorgchem.9b01238
*Inorg. Chem.* 2019, 58, 10871−10882

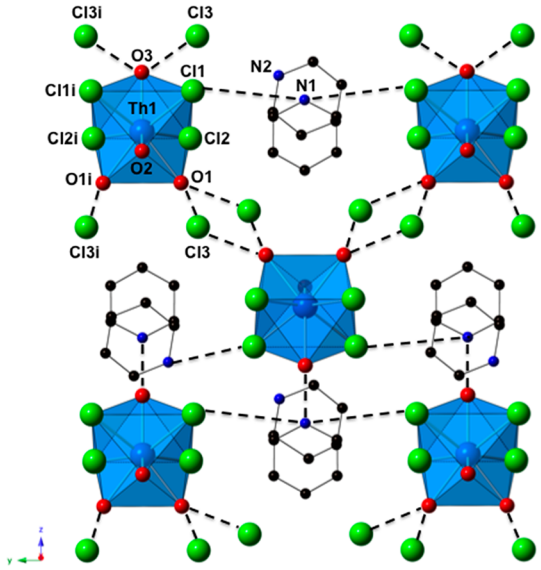


**Figure 1.** Packing diagram of **1** highlighting the supramolecular interactions (dotted black lines) between the $Th(H_2O)_4Cl_4$ structural unit and the outer coordination sphere pyridinium and chloride ions. $\pi-\pi$ stacking interactions are also present, although not shown. H atoms and disorder of the pyridinium rings are omitted for clarity (Th = light blue, Cl = light green, O = red, *N* = dark blue, C = black). Symmetry equivalent atoms were generated through their respective symmetry elements ($i = x, -y + {}^1/_2, z$).

three ligated chlorides, one water molecule, two $\mu_2$-hydroxides with Th2−O1/O3 distances of 2.387(2) and 2.343(2) Å, and two $\mu_3$-hydroxides with Th2−O2 distances of 2.478(2) and 2.507(3) Å. Overall, the Th atoms of the $[Th_3(OH)_5]^{7+}$ core lie in a single plane linked through three $\mu_2$-OH groups which bend away from the center of the cluster. Two remaining $\mu_3$-OH groups bridge all three Th atoms in the middle of the cluster. In contrast to the $\mu_2$-OH groups that lie in plane with the Th metal centers, these $\mu_3$-OH groups pucker above and below the plane. Similar to the monomer in **1**, the calculated bond distances for the trimer in **2** are longer than experiment. The Th1−O1 distances for the $\mu_2$-hydroxides are calculated to be 2.46 Å and the $\mu_3$-hydroxides have Th1−O2 distances of 2.63 and 2.65 Å. Th2−O(4)$H_2$ distances are calculated to be 2.74 Å; the two $\mu_2$-hydroxides have Th2−O1 distances of 2.30 Å where the OH bonds to Th1. The other $\mu_2$-hydroxide (O3) that completes the trimeric unit yields a Th2−O3 distance of 2.38 Å. The $\mu_3$-hydroxides are calculated to be about 2.47−2.48 Å. The calculated Th−Cl bond distances range from 2.74−2.92 Å.

The anionic trinuclear building unit $[Th_3(H_2O)_2Cl_{10}(OH)_5]^{3-}$ exists in **2** as an isolated molecular unit, capped by ligated chloride and water molecules. Seven pyridinium and four chloride ions exist in the outer coordination sphere to charge-balance the trimeric unit (Figure 2b). Outer coordination sphere chloride anions and pyridinium cations together engage in the shortest H-bonding interactions present in **2** with N-(H)···Cl distances ranging from 3.017(19) to 3.445(13) Å. Pyridinium cations further engage in H-bonding interactions with bound chlorides of the trimeric structural unit, yielding distances of N2-(H)···Cl1 = 3.193(6) Å and N4-(H)···Cl6 = 3.332(14) Å respectively. Similar to **1**, the strength of H-bonding interactions present in **2** can be classified as moderate to weak.[60] $\pi-\pi$ stacking interactions yielded a $C_{HPy}\cdots C_{HPy}$ distance of 3.8547(3) Å and a slip angle of 30°.

**Vibrational Spectroscopy.** Density functional theory calculations allowed for predictions of the vibrational properties of **1** and **2**; subsequent comparisons to experimental findings are discussed below.

The IR spectra for **1** and **2** exhibited many similar features that are attributed to the presence of pyridinium cations in the outer coordination sphere for both compounds (Figure 3), particularly between 400 and 1650 $cm^{-1}$. The presence of water in both compounds was additionally confirmed via IR. In **1**, the $H_2O$ H−O−H bends were experimentally observed at 1616 $cm^{-1}$ with the corresponding computational H−O−H bends for the four $H_2O$ molecules calculated to fall between 1540 and 1645 $cm^{-1}$. The experimental band at 543.5 $cm^{-1}$ is assigned to motions of the $H_2O$ group and there are

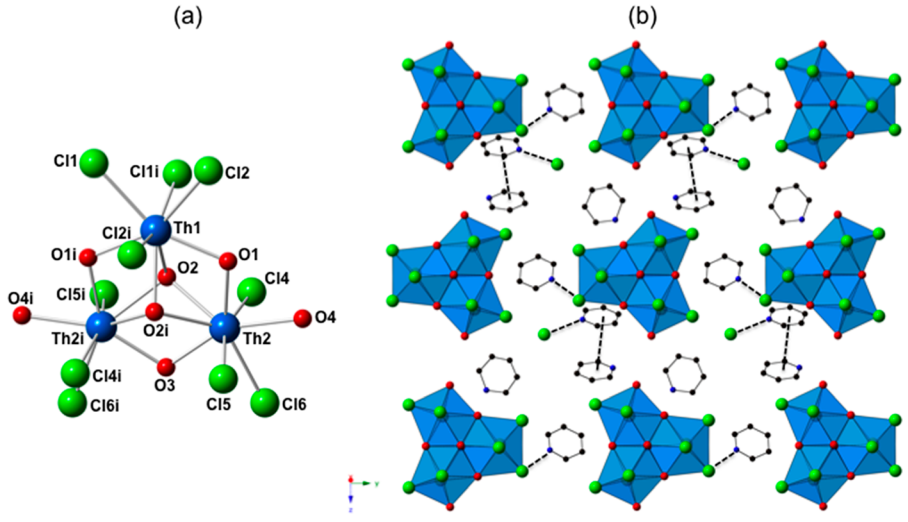


**Figure 2.** (a) $[Th_3(H_2O)_2Cl_{10}(OH)_5]^{3-}$ structural unit in **2**. (b) Packing diagram of **2** highlighting isolated trimers and interstitial pyridinium cations and chloride ions. Supramolecular interactions are highlighted by dotted black lines. H atoms and disorder of the pyridinium rings are omitted for clarity (Th = light blue, Cl = light green, O = red, N = dark blue, and C = black). Symmetry equivalent atoms were generated through their respective symmetry elements ($i = -x + 1, y, -z + {}^1/_2$).



DOI: 10.1021/acs.inorgchem.9b01238
*Inorg. Chem.* 2019, 58, 10871−10882

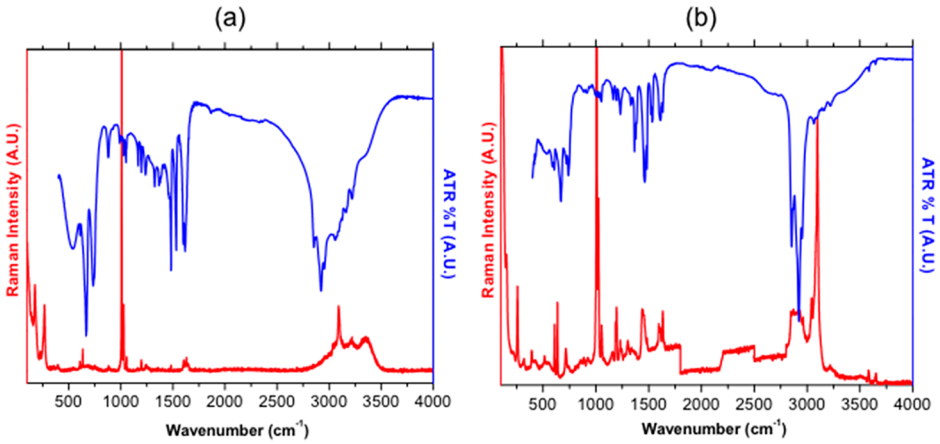


**Figure 3.** Infrared and Raman spectra of compounds **1** (a) and **2** (b). (Raman = red, IR = blue). Difference in background intensity, observed as steps, over 1750−2750 $cm^{-1}$ in the Raman spectrum of **2** resulted from instability of the crystals under prolonged laser exposure.

corresponding calculated values in this spectral region (Table S2). The OH stretches of the $H_2O$ molecules are experimentally observed at 3401 $cm^{-1}$ in the solid and are red-shifted as compared to the calculated values due to intermolecular H-bonding; the computational results for the isolated gas phase molecule fall within the range of 3635−3879 $cm^{-1}$, typical of a free $H_2O$ molecule. In **2**, vibrations attributed to the presence of bound water are likewise observed. The calculated OH stretches for the $H_2O$ molecules are found from 3540 to 3616 $cm^{-1}$ and are considerably red-shifted from the $H_2O$ OH stretches in **1**. Furthermore, $\mu_2$-OH or $\mu_3$-OH experimental vibrations could possibly be assigned at 3736 and 3586 $cm^{-1}$, although the intensity of these peaks is weak. One of the crystallographically unique $\mu_2$-hydroxides is predicted to be at 3869 $cm^{-1}$ and the other unique $\mu_2$-hydroxide is at 3815 $cm^{-1}$, while the $\mu_3$-hydroxides are predicted at 3775 $cm^{-1}$. These results are consistent with prior work that assigned Th−$\mu_2$-OH or Th−$\mu_3$-OH IR stretches between 2500 and 3700 for Th−selenate oligomers[63] and Th−$\mu_3$-OH stretches for Th hexamers, which were calculated to fall between 3806 and 3815 $cm^{-1}$.[29]

The Raman spectra of **1** and **2** show clear differences (Figure 3). Above 1000 $cm^{-1}$, peaks attributed to pyridinium, symmetric/asymmetric −OH stretches, and H−O−H bending modes of water are present in both spectra. The most intense peaks at 1008, 1028, 1056, 3039, and 3095 $cm^{-1}$ for **1** and 1007, 1026, 1055, 3042, and 3098 $cm^{-1}$ for **2** are consistent with pyridine in 10% HCl; shifts of these stretches in comparison to the spectrum of neat pyridine are attributed to pyridinium acting as a Brönsted acid in **1** and **2**.[64] The presence of water in both complexes is also confirmed by Raman spectroscopy, with the bands between 1600−1640 $cm^{-1}$ arising from the bending mode of $H_2O$. Characteristic C═N stretches of pyridinium are likewise observed in this region. Lastly, the OH stretches are observed as a broad band centered at 3354 $cm^{-1}$ in **1**, and there are two distinct peaks at 3580 and 3652 $cm^{-1}$ in **2**. Lower wavenumbers for the OH stretches of the $H_2O$ molecules compared to more commonly reported values are likely due to extensive H-bonding present in both structures.[65−68]

As shown in Figure 3, mixed Th−O($H_2$)/Th−Cl vibrations are experimentally observed between 200−400 $cm^{-1}$. For **1**, the most intense peak within this range is found at 258 $cm^{-1}$ in comparison to the most intense computationally predicted peak at 313 $cm^{-1}$. Other Th−O($H_2$)/Th−Cl vibrations are observed at 220 and 322 $cm^{-1}$. The spectrum for **2** shows that there is reasonable agreement between experiment and computation; mixed Th−O($H_2$)/Th−Cl vibrations are experimentally observed at 228 and 265 $cm^{-1}$ for **2**, and computationally predicated at 221 and 265 $cm^{-1}$, respectively. $H_2O$ group inversions are observed at 393 $cm^{-1}$ for both compounds. Pyridinium stretches are also present in this range for both compounds, predicted at 618 and 641 $cm^{-1}$ and observed experimentally in both **1** and **2** at 609/637 $cm^{-1}$ (**1**) and 607/634 $cm^{-1}$ (**2**) respectively. There is one vibration present in **2** but not in **1** - a broad peak centered at 716 $cm^{-1}$. This can be assigned as a $\mu_3$-OH bend. Computationally, multiple vibrations were predicted in this range at 712, 715, and 726 $cm^{-1}$ (most intense) and likely would fall under the broad peak observed experimentally.

Of the thorium oligomers reported, Raman assignments for $\mu_2$-hydroxides have been reported for Th(IV)−selenate clusters built from $[Th_8(\mu_2\text{-}OH)_8(\mu_3\text{-}O)_4]^{16+}$ cores; however, these were not differentiated from −OH vibrations attributed to water in the structures.[36] In contrast, Raman assignments for $\mu_3$-hydroxides are much more well studied due, in part, to the number of Th hexanuclear clusters that have been isolated.[27,28,30,31] In particular, a combined experimental/computational investigation regarding the Raman behavior of several Th hexamers with the general formula $Th_6(\mu_3\text{-}OH)_4(\mu_3\text{-}O)_4]^{12+}$ predicted a $\mu_3$-OH bend between 666 and 750 $cm^{-1}$; the $\mu_3$-OH bend was experimentally observed at 706, 711, and 750 $cm^{-1}$ based on the ligands decorating the clusters.[29] This prior study is consistent with the results for **2** in this work. A $\mu_3$-OH stretch was also computationally predicted to exist for the Th hexamers between 3806−3815 $cm^{-1}$ (as discussed in the IR section, *vide supra*) but was never experimentally observed, similar to the absence of this peak in the Raman spectrum of **2**. However, the two distinct peaks at 3580 and 3652 $cm^{-1}$ in **2** could arguably be assigned as $\mu_2$-OH or $\mu_3$-OH stretches, experiencing hypsochromic shifts like those observed in the IR spectra due to H-bonding in the structure.[65,69] Overall, there is agreement between the calculated and observed vibrations in both Raman and IR spectra. The presence of a peak at 716 $cm^{-1}$ assigned to a $\mu_3$-hydroxide bend distinctly differentiates **1** from **2** while also confirming the presence of this structural functionality within the trimeric structural unit.



DOI: 10.1021/acs.inorgchem.9b01238
*Inorg. Chem.* 2019, 58, 10871−10882

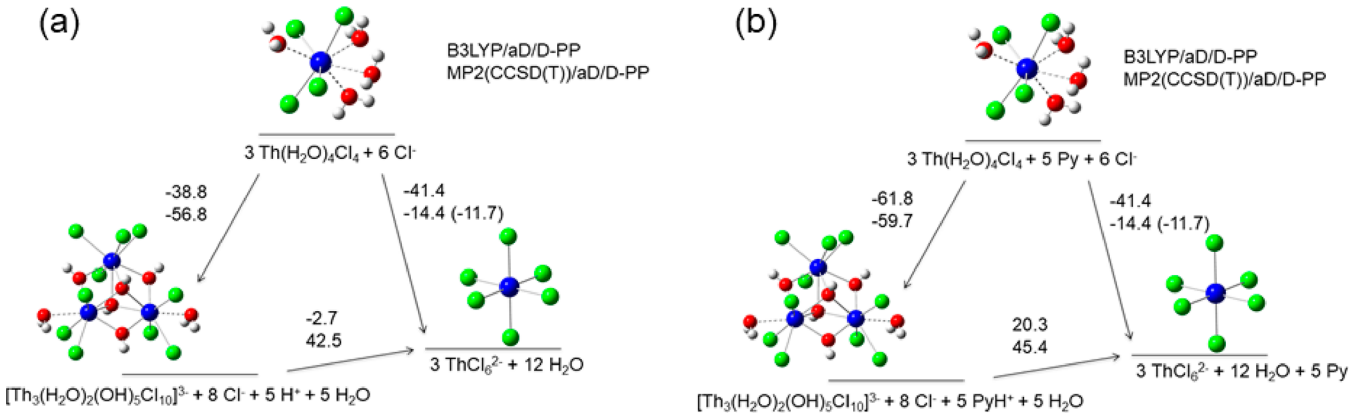


**Figure 4.** Reaction free energies in aqueous solution at 298 K in kcal/mol for the reaction of the monomer in **1** to form the trimer in **2** and $ThCl_6^{2-}$ in the (a) absence and (b) presence of pyridine. For each reaction, the top number corresponds to the value of the free energy in aqueous solution obtained at the B3LYP/aD/D-PP level. The bottom number corresponds to the value of the free energy in aqueous solution obtained at the MP2/aD/D-PP level with the corresponding CCSD(T) values in parentheses. See text for exact details of the calculations. Th is blue, Cl is green, O is red, and H is white.

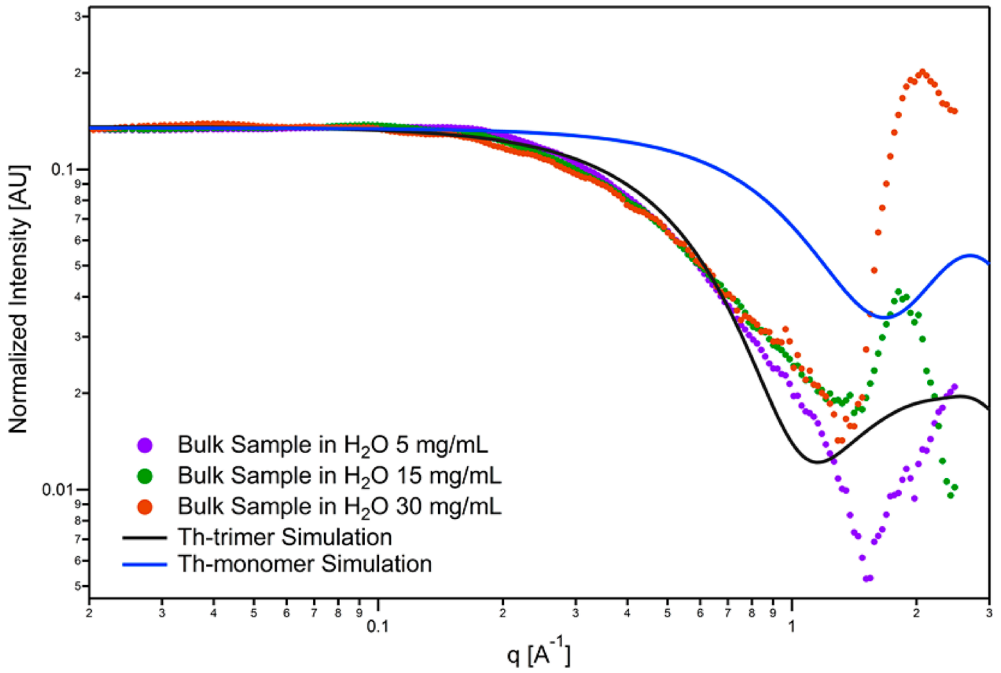


**Figure 5.** Comparison of the normalized-intensity $\log(q)-\log(I(q))$ scattering curves of the bulk reaction product, containing **1** and **2**, dissolved in water at 5 (purple), 15 (green), and 30 (red) mg of bulk sample/mL of $H_2O$. The simulated scattering curves for the monomer in **1** (blue) and the trimer in **2** (black) are shown for reference. Normalization allows for ease in comparing the Guinier regions.

**Reaction Energetics.** To predict the energetics of **1** relative to **2**, calculations were performed to assess the transformation from the monomer to the trimer. Additionally, calculations included the octahedral $ThCl_6^{2-}$ dianion, as $AnCl_6^{2-}$ (An = U, Np, Pu) complexes are quite prevalent in the literature and are common products that precipitate from solutions of An(IV) ions in hydrochloric acid, yet $ThCl_6^{2-}$ is not observed in our reaction products.[10]

For the reaction of $Th(H_2O)_4Cl_4$ to form $ThCl_6^{2-}$, benchmark calculations were done at the CCSD(T) level to check the values obtained at the MP2 and DFT/B3LYP levels. The CCSD(T) calculations could not be performed for the trimer as they scale as $N^7$, with $N$ equal to the number of basis functions. The MP2 calculations are in better agreement with the higher level CCSD(T) calculations, which serve as a benchmark, than are the DFT/B3LYP values. Therefore in the discussion below, we focus on the MP2 values. Note that all of these values are free energies in aqueous solution ($\Delta G_{aq}$) obtained using gas phase free energies and the free energy of solvation from a self-consistent reaction field calculation (eq 1). Our approach is based on that used to study the reaction of $U(H_2O)_4Cl_4$ to form $UCl_6^{2-}$.[10] The reaction from the Th–aquo–chloro monomer to the $ThCl_6^{2-}$ dianion is predicted to be exothermic, −4 kcal/mol at the CCSD(T) level and −5 kcal/mol at the MP2 level. Note that the values in Figure 4 for this reaction are multiplied by 3 in order to be compatible with formation of the trimer. The CCSD(T) value is slightly more exothermic than the corresponding value of −1 kcal/mol for the same reaction with uranium instead of Th.



DOI: 10.1021/acs.inorgchem.9b01238
Inorg. Chem. 2019, 58, 10871−10882

We can consider two ways to write the reaction of the monomer to form the trimer. The first is with formation of pure protons and the second is in the protons trapped by pyridinium. At the MP2 level, there is very little difference due to the presence of pyridine, and the reaction is predicted to be very exothermic to form the trimer. As shown in Figure 4, the reaction to form the trimer is substantially more exothermic than it is to form $ThCl_6^{2-}$, consistent with the lack of experimental observation of $ThCl_6^{2-}$.

The specific reaction for the trimer was chosen to make it as close as possible to the types of atoms present in formation of the Th hexachloride dianion. There are many more species in solution and it would be difficult to exhaustively know all of the possible reaction channels. Although the reaction from the monomer is predicted to be highly exoergic for the reaction as written, it does not mean that there are not other competing pathways that could take the trimer back to the monomer as found experimentally. Note that these reaction energies are only for reactions in aqueous solution and do not include the presence of a solid phase or any effects of counterions and pH.

**Small Angle X-ray Scattering Studies.** The solution phase stability of the reported compounds was examined using SAXS. X-ray data were collected on the bulk sample dissolved in aqueous solution at three different concentrations and compared to the simulated scattering curves for monomeric and trimeric units observed in **1** and **2**, respectively (Figure 5). Qualitatively, at all concentrations, the experimental scattering curves resemble the general shape of the simulated scattering curve calculated for the trimeric unit, particularly in the Guinier region ($q$ = 0.2−0.6 Å$^{-1}$). Thus our initial assessment suggests the trimeric structural unit remains intact when redissolved in water, or monomers present also assemble to trimeric units upon dissolution in neat water, without excess acid. On the other hand, the mismatch between the simulated (trimer) and experimental data, observed by the rise in scattering intensity between $q$ = 0.7 and 1.3 Å$^{-1}$, potentially indicative of a Guinier region at high $q$-value, suggested the presence of smaller species. To investigate the presence of the monomer form, we applied a 2-phase model to the data in which we fit the curves with form factors for both the monomer and the trimer. The result of these attempts can be interpreted as (1) there is minimal monomer present in solution, (2) the monomer scattering is too weak to be detected in the presence of the trimer (scattering intensity is proportional to radius$^6$), or (3) the excess scattering at higher $q$ is attributed to scattering by the $Cl^-$ ions, since the mismatch increases with increasing concentration (Figure S8). It is likely a combination of all three. However, the scattering intensity in the low-$q$ plateau region (below q = 0.1 Å$^{-1}$) increases with decreasing concentration. We suspect this is because any monomers present convert to trimers, since decreasing concentration increases the self-buffering pH, driving hydrolysis/condensation reactions. The increased scattering from conversion of smaller to larger species overwhelms the decrease in scattering from total concentration of species (intensity scales linearly with total concentration, compared to exponentially with species volume).

Using Modeling II macros in Irena with a single-phase fit, we determined the radii of the approximately spherical particles present in the three different concentrations (Table 2). The radius of gyration ($R_g$, a shape independent root-mean-squared sum of scattering vectors through the particles) value is directly correlated to the radius of the dissolved species ($1.29 \times R_g \approx R$; $R$ = radius of approximately spherical species). The experimentally determined radii (and derived $R_g$ values) are in agreement with the calculated values, confirming the trimer stays intact upon dissolution, and the solutions are dominated by the trimer species. Interestingly, the average radius of scattering species increases slightly with increasing concentration, despite the monomer to trimer conversion. We attribute this to increased ion-association between the chloride anions and thorium cationic species with increased concentration.

**Table 2. Summary of the Modeling II Fits of the Bulk Sample and the Calculated Values**

| sample | $R$ (Å) | $R_g$ (Å)[a] |
|---|---|---|
| simulated trimer | 5.24 | 6.76[b] |
| 5 mg/mL | 5.12 | 6.60 |
| 15 mg/mL | 5.28 | 6.82 |
| 30 mg/mL | 5.38 | 6.94 |

[a]Calculated from experimental $R$ ($R/1.29 \approx R_g$, $R$ = radius of approximately spherical species). [b]Determined from SolX.

## DISCUSSION

**Monomeric Actinide Chlorides.** An halides, and An−Cl compounds in particular, have broadly been explored for many decades due to their relevance to waste management and separations chemistry, their role in probing covalency in the f-block, and their utility as starting materials for transuranic syntheses.[3,70,71] For the tetravalent An ions, there are a number of $AnCl_6^{2-}$ (An = U, Np, Pu) based structures reported that are charge balanced by numerous cations and crystallized under a range of synthetic conditions.[10,59,72−76] In contrast, there are only a few reports of $ThCl_6^{2-}$ compounds.[59,72,77]

There is clearly precedence for $AnCl_6^{2-}$ structural units, yet it is worth highlighting that only a few solid-state examples of An−aquo−halide compounds have been described, despite their identification in solution and by electronic structure predictions.[78,79] The Th−aquo−chloro compound reported in this work is isomorphous to a previously reported U(IV)−aquo−chloro complex.[10] Further, Kiplinger et al. isolated a $Th(H_2O)_4Cl_4$ structural unit recrystallized from tetrahydrofuran or 1,4-dioxane by refluxing $Th(NO_3)_4{\cdot}(H_2O)_5$ at elevated temperatures in 12 M HCl.[80] Kiplinger's $Th(H_2O)_4Cl_4{\cdot}(1,4\text{-dioxane})_3$ and $Th(H_2O)_4Cl_4{\cdot}(THF)_5$ compounds exhibit a different coordination about the metal center, displaying a distorted square antiprism geometry. Related monomeric and dimeric An−aquo−halide compounds that only contain water or chloride in their first coordination sphere have also been reported.[81,82] Notable reports for monomeric Th(IV) include the homoleptic $[Th(H_2O)_{10}]^{4+}$ structural unit, which was isolated from HBr solution, crystallizing with four bromide ions in the outer coordination sphere, and $[Th(H_2O)_7Cl_2]{\cdot}Cl_2{\cdot}$18-crown-6$\cdot 2H_2O$.[58,83] Monomeric Pu(III)−aquo−chloro complexes have also been reported with varying aquo/chloride ratios and counterions including *cis*-$Cs[Pu(H_2O)_4Cl_4]$, *trans*-$Cs_5[Pu(H_2O)_4Cl_4]Cl_4{\cdot}2H_2O$, $(Et_4N)[Pu(H_2O)_6Cl_2]Cl_2{\cdot}2H_2O$, and $(C_5H_5NBr)_2[Pu(H_2O)_5Cl_3]Cl_2{\cdot}2H_2O$.[84,85] Furthermore, dimeric hydrolysis products have been isolated, including $[Th(\mu_2\text{-}OH)_2Cl_2(H_2O)_{12}]Cl_4{\cdot}2H_2O$ from acidic HCl solutions and $[Th(\mu_2\text{-}OH)Cl(H_2O)_6]_2Cl_4{\cdot}$18-crown-6$\cdot 2H_2O$ stabilized by 18-crown-6 molecules.[17,80]

The extensive library of $AnCl_6^{2-}$ (An = U, Np, and Pu) compounds coupled with the limited reports of $ThCl_6^{2-}$ point



DOI: 10.1021/acs.inorgchem.9b01238
Inorg. Chem. 2019, 58, 10871−10882

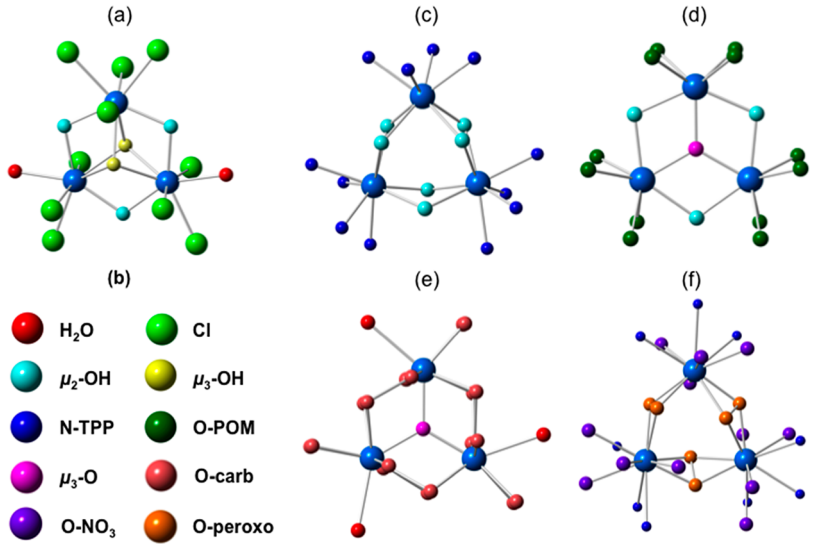


**Figure 6.** Comparison of trinuclear building units observed in various compounds, highlighting different ligand environments. (a) Trimeric unit in $(HPy)_3[Th_3(H_2O)_2Cl_{10}(OH)_5]\cdot 4(HPy\cdot Cl)$ (**2**) reported herein. (b) Color code representing different types of ligands found in trimeric structural units (O-POM = oxygens bound to the polyoxometalate unit, $[SiW_9O_{34}]^{10-}$, O-carb = oxygens bound to carboxylates, N-TPP = nitrogens bound to tetraphenylporphyrin or 2,2′:6′,2″-terpyridine). $Th_3$ structural units observed in (c) $[(TPP)Th(\mu_2\text{-}OH)_2]_3\cdot 2H_2O\cdot 3C_7H_{16}$[22] (TPP = tetraphenylporphyrin), (d) $Na_{12}Rb[Th_3(\mu_3\text{-}O)(\mu_2\text{-}OH)_3(SiW_9O_{34})_2]$,[23] (e) $[Th_3(\mu_3\text{-}O)(BTC)_3(OH)(H_2O)_2]\cdot 2.9DMF\cdot 1.5H_2O$[24] (BTC = 1,3,5-benzentricarboxylate) and $[Th_3(\mu_3\text{-}O)\text{-}(bptc)_3(H_2O)_{3.78}]\cdot Cl\cdot(C_5H_{14}N_3Cl)\cdot 8H_2O$[25] (bptc = [1,1-biphenyl]-3,4,5-tricarboxylate), and (f) $[Th(\mu\text{-}\eta^2\text{:}\eta^2\text{-}O_2)(terpy)(NO_3)_2]_3$[91] (Th =light blue).

toward a break in the structural chemistry of the early actinides. As highlighted in this work, only $Th(H_2O)_4Cl_4$ is observed. When compared to U(IV) under identical reaction conditions as those reported here, it was found that U(IV) formed $(HPy)_2UCl_6$ exclusively.[10] It was only upon the addition of a noncomplexing amino acid that the formation of the $U(H_2O)_4Cl_4$ structural unit was observed. Similarly, in the separations community it has been known for decades that the anion exchange behavior of Th(IV) in hydrochloric acid is different than that of the other tetravalent An ions (U, Np, Pu).[86] Even in concentrated HCl, Th(IV) adsorption to a strong base quaternary amine resin is found to be negligible.[86] In contrast, U(IV) exhibits minimal adsorption to the resin below 5.5 M HCl but rapidly increased with increased HCl concentrations, consistent with the formation of $UCl_6^{2-}$ and its subsequent interaction with the resin as an anion.[86] For Np(IV) and Pu(IV), with decreasing ionic radii, higher concentrations of $AnCl_6^{2-}$ form at lower concentrations of HCl.[87] Under the conditions used for anion exchange, it is likely thorium forms a Th−aquo−chloro derivative that is not anionic, thereby prohibiting its adsorption to the resin. The propensity of Th to form aquo−chloro complexes versus the tendency of the later actinides to form $AnCl_6^{2-}$ units likely arises from disparities in ionic radii between An(IV) metals. Due to its larger size, Th forms higher coordinate complexes and the hexacoordinate $ThCl_6^{2-}$ complex is not easily isolated or observed. Consistent with this point are observations that Th salts are quite hygroscopic, and as a result the isolation of anhydrous Th compounds from acidic aqueous solution is challenging, accounting for the limited reports of Th hexachlorides.[77,88]

**Trimeric Thorium Hydrolysis Products.** In addition to the isolation of the monomeric Th(IV)−aquo−chloro complex, the trimeric compound reported herein is, to the best of our knowledge, the first report of a $[Th_3(OH)_5]^{7+}$ unit isolated from aqueous solution. A few trinuclear building blocks for Th have been previously reported;[22−25,89−91] however, **2** presented herein exhibits a novel Th coordination and extended topology. Comparison of **2** with other reported trimeric units is displayed in Figure 6. In 1988, the first isolation of a trimeric species came under nonaqueous conditions from Kadish and co-workers in which three eight-coordinate Th cations are bridged by six $\mu_2$-hydroxo ligands.[22] The $[Th_3(\mu_2\text{-}OH)_6]^{6+}$ core is stabilized by tetraphenylporphyrin ligands, resulting in the first report of a trimeric metalloporphyrin (Figure 6c). Almost three decades later, Duval et al. identified a Th(IV) trinuclear building block isolated from acetate buffer.[23] The $[Th_3(\mu_2\text{-}OH)_3(\mu_3\text{-}O)]^{7+}$ core is built from three seven-coordinate Th metal centers bridged through $\mu_2$-hydroxides and a central $\mu_3$-oxo. The trimeric structural unit presented in Figure 6d is sandwiched between $[\alpha\text{-}SiW_9O_{34}]^{10-}$ polyoxometalates. Next are two trinuclear building units bridged by carboxylate ligands to form multidimensional coordination polymers that were synthesized solvothermally/ionothermally by Martin et al. and Li et al., respectively (Figure 6e).[24,25] Martin and co-workers reported a $[Th_3(\mu_3\text{-}O)(BTC)_3]^+$ (BTC = 1,3,5-benzentricarboxylate) core that contains a 10-fold coordination environment about the Th metal and displays a single $\mu_3$-oxo in the center of the cluster. The trimeric building unit is linked to adjacent trimers through BTC ligands, yielding an open-framework coordination polymer. Li and co-workers presented a similar trinuclear building unit $[Th_3(\mu_3\text{-}O)(bptc)_3]^+$ (bptc = [1,1′-biphenyl]-3,4′,5-tricarboxylate) that formed a 3D cationic framework. The trimer reported herein differs from these four complexes in that the structural units in **2** exist as isolated molecular complexes and are not bridged into an extended network. Additionally, the trimer was not isolated with stabilization from polyoxometalates or porphyrin ligands. The synthetic approach used in this work may stabilize the $Th_3(\mu_3\text{-}OH)_2$ moiety, which has unique connectivity and is notably different from the single $\mu_3$-oxo bridged $Th_3$ clusters



DOI: 10.1021/acs.inorgchem.9b01238
Inorg. Chem. 2019, 58, 10871−10882

that have previously been reported.[23−25] Other related trimeric structural units include a trimeric Th hydride,[89] $Th_3(\mu_3\text{-}H)_2(\mu_2\text{-}H)_4(OAr)_6$ (Ar = 2,6-*t*-$Bu_2C_6H_3$), a Th-MOF containing $Th[C_6H_3(CO_2)_3F]\cdot 0.3H_2O$ units,[90] and a trimeric Th peroxide cluster,[91] $[Th_3(\mu\text{−}\eta^2\text{:}\eta^2\text{-}O_2)(terpy)_3(NO_3)_6]\cdot 3CH_3CN$ (Figure 6f, terpy = 2,2′:6′,2′′-terpyridine).

Thermodynamic studies do not predict the $Th_3$ structural unit to exist in noncomplexing media over a pH range of 1−14.[3] Instead, only $Th^{4+}$, $[Th(OH)_x]^{y+}$, $[Th_2(OH)_2]^{6+}$, $[Th_4(OH)_8]^{8+}$, and $[Th_6(OH)_{15}]^{9+}$ are proposed.[92,93] Monomers, dimers, tetramers, hexamers, octamers, and even a decamer are established in the solid-state for thorium.[17−21,26,27,31,35−37,94−96] Thus, the isolation of **2** as a trimeric unit from aqueous solution illustrates the novelty of this complex. Of the previously reported trimers, Kadish et al. established the persistence of the trimeric unit with a chelating porphyrin ligand in solution by NMR; Li and co-workers observed their Th MOF in aqueous solutions through hydrolytic stability measurements.[22,25] Other reports did not identify the trimer in solution. In this work, Raman spectroscopy was used to monitor the reaction solution until crystallization occurred (Figure S5). Evidence supporting the assembly of the trimer; however, was not observed as the spectra are dominated by water and pyridinium signatures. However, dissolution of **2** in aqueous solution and subsequent analysis by small-angle X-ray scattering showed that the trimeric structural unit remained intact in water.

The isolation of **2** in the solid-state may be due to the high concentration of Th(IV) in the reaction, as increased concentration of the metal is well-known to favor hydrolysis and condensation chemistries.[5] Alternatively the isolation of **2** may be attributed to the high ionic strength of the solution or additionally to the presence of outer coordination sphere molecules (pyridinium) that engage in noncovalent interaction to stabilize and precipitate the structural unit. In any case, the isolation of **2** under highly acidic conditions not only highlights thorium's ability to form trimeric units without chelating and complex organic ligands (i.e., porphyrin rings or carboxylates) but also supports the trimer as an accessible species that exists in nuclearity between mononuclear species and the ultimate thermodynamic product, $ThO_2$.

## CONCLUSIONS

The evaporation of an acidic aqueous solution containing Th and pyridinium resulted in the formation of two novel phases, $[Th(H_2O)_4Cl_4]\cdot 2(HPy\cdot Cl)$ (**1**) and $(HPy)_3[Th_3(H_2O)_2Cl_{10}(OH)_5]\cdot 4(HPy\cdot Cl)$ (**2**), which consisted of monomeric and trimeric Th structural units, respectively. To the best of our knowledge, this is the first report of a trimeric Th−hydroxo bridged unit isolated from aqueous solution absent more complex stabilizing ligands such as carboxylates, polyoxometallates, or porphyrins. Single crystal X-ray diffraction data for both phases is reported, along with assignment of Raman and IR vibrational modes. Electronic structure calculations showed an energetic driving force toward the trimeric unit from $Th(H_2O)_4Cl_4$ and its presence in solution was established using small-angle X-ray scattering. The pyridinium cations present in the reaction solution may facilitate the crystallization of **2** by engaging in noncovalent interactions and highlights an important synthetic strategy that may be used to isolate otherwise elusive metal complexes and clusters. Importantly, observation of the trimeric unit in the solid-state *and* solution provides evidence for a species that was largely absent from descriptions of the hydrolysis and condensation chemistry of Th, and it may have significant implications for understanding the aqueous phase behavior of Th.

## ASSOCIATED CONTENT

### Supporting Information

The Supporting Information is available free of charge on the ACS Publications website at DOI: 10.1021/acs.inorgchem.9b01238.

ORTEP diagrams, powder X-ray diffraction patterns, bond valence summation calculations, solution Raman spectra, calculated frequencies ($cm^{-1}$), IR intensities (km/mol), Raman activity ($Å^4$/amu), results of electronic structure calculations including optimized coordinates, and non-normalized scattering curves (PDF)

### Accession Codes

CCDC 1904843−1904844 contain the supplementary crystallographic data for this paper. These data can be obtained free of charge via www.ccdc.cam.ac.uk/data_request/cif, or by emailing data_request@ccdc.cam.ac.uk, or by contacting The Cambridge Crystallographic Data Centre, 12 Union Road, Cambridge CB2 1EZ, UK; fax: +44 1223 336033.

## AUTHOR INFORMATION


### Corresponding Author

*(K.E.K.) E-mail: kek44@georgetown.edu.

### ORCID

Jeffery A. Bertke: 0000-0002-3419-5163
May Nyman: 0000-0002-1787-0518
David A. Dixon: 0000-0002-9492-0056
Karah E. Knope: 0000-0002-5690-715X


### Notes

The authors declare no competing financial interest.

## ACKNOWLEDGMENTS

The primary source of support for this work is the U.S. Department of Energy, Office of Science, Office of Basic Energy Sciences, Early Career Research Program under Award DE-SC0019190. The syntheses and characterization of the Th phases were performed at Georgetown University by J.N.W. and K.E.K., supported under this award. The authors also thank the National Science Foundation under Grants NSF CHE-1429079 and NSF CHE-1337975 for SCXRD and Raman instrumentation, respectively. D.A.D. and M.V. were supported by the U.S. Department of Energy, Office of Basic Energy Sciences, Chemical Sciences, Geosciences, & Biosciences Division, Heavy Element Chemistry Program, (DE-SC0018921). D.A.D. thanks the Robert Ramsay Fund at The University of Alabama for support. The SAXS studies were performed at Oregon State University by I.C. and M.N. who are supported by the Department of Energy, National Nuclear Security Administration, under Award Number DE-NA0003763. The authors also thank Dr. Stosh Kozimor for insightful discussions regarding separation efforts of the actinides in hydrochloric acid.

## REFERENCES

(1) Baes, C. F.; Mesmer, R. E. *Hydrolysis of cations*. Wiley: 1976.



DOI: 10.1021/acs.inorgchem.9b01238
*Inorg. Chem.* 2019, 58, 10871−10882

(2) Maher, K.; Bargar, J. R.; Brown, G. E. Environmental Speciation of Actinides. *Inorg. Chem.* **2013**, *52*, 3510−3532.
(3) Katz, J. J.; Morss, L. R.; Edelstein, N.; Fuger, J. *The Chemistry of the Actinide and Transactinide Elements*, 3rd ed.; Springer Netherlands: 2007; Vols *1*−*5*).
(4) Clark, S.; Buchanan, M.; Wilmarth, B. *Basic Research Needs for Environmental Management (No. PNNL-25166)*; Pacific Northwest National Lab (PNNL): Richland, WA, 2016.
(5) Knope, K. E.; Soderholm, L. Solution and Solid-State Structural Chemistry of Actinide Hydrates and Their Hydrolysis and Condensation Products. *Chem. Rev.* **2013**, *113*, 944−994.
(6) Loiseau, T.; Mihalcea, I.; Henry, N.; Volkringer, C. The crystal chemistry of uranium carboxylates. *Coord. Chem. Rev.* **2014**, *266*−*267*, 69−109.
(7) Hu, Y.-J.; Knope, K. E.; Skanthakumar, S.; Soderholm, L. Understanding the Ligand-Directed Assembly of a Hexanuclear $Th^{IV}$ Molecular Cluster in Aqueous Solution. *Eur. J. Inorg. Chem.* **2013**, *2013*, 4159−4163.
(8) Li, P.; Wang, X.; Otake, K.-i.; Lyu, J.; Hanna, S. L.; Islamoglu, T.; Farha, O. K. Synthetic Control of Thorium Polyoxo-Clusters in Metal−Organic Frameworks toward New Thorium-Based Materials. *ACS Applied Nano Materials* **2019**, *2*, 2260.
(9) Li, P.; Goswami, S.; Otake, K.-i.; Wang, X.; Chen, Z.; Hanna, S. L.; Farha, O. K. Stabilization of an Unprecedented Hexanuclear Secondary Building Unit in a Thorium-Based Metal-Organic Framework. *Inorg. Chem.* **2019**, *58*, 3586.
(10) Wacker, J. N.; Vasiliu, M.; Huang, K.; Baumbach, R. E.; Bertke, J. A.; Dixon, D. A.; Knope, K. E. Uranium(IV) Chloride Complexes: $UCl_6^{2-}$ and an Unprecedented $U(H_2O)_4Cl_4$ Structural Unit. *Inorg. Chem.* **2017**, *56*, 9772−9780.
(11) Jin, G. B.; Lin, J.; Estes, S. L.; Skanthakumar, S.; Soderholm, L. Influence of Countercation Hydration Enthalpies on the Formation of Molecular Complexes: A Thorium−Nitrate Example. *J. Am. Chem. Soc.* **2017**, *139*, 18003−18008.
(12) Estes, S. L.; Qiao, B.; Jin, G. B. Ion association with tetra-n-alkylammonium cations stabilizes higher-oxidation-state neptunium dioxocations. *Nat. Commun.* **2019**, *10*, 59.
(13) Hou, Y.; Zakharov, L. N.; Nyman, M. Observing Assembly of Complex Inorganic Materials from Polyoxometalate Building Blocks. *J. Am. Chem. Soc.* **2013**, *135*, 16651−16657.
(14) Antonio, M. R.; Nyman, M.; Anderson, T. M. Direct Observation of Contact Ion-Pair Formation in Aqueous Solution. *Angew. Chem., Int. Ed.* **2009**, *48*, 6136−6140.
(15) Abeysinghe, S.; Unruh, D. K.; Forbes, T. Z. Crystallization of Keggin-Type Polyaluminum Species by Supramolecular Interactions with Disulfonate Anions. *Cryst. Growth Des.* **2012**, *12*, 2044−2051.
(16) Allen, F. H. The Cambridge Structural Database: a quarter of a million structure and rising. *Acta Crystallogr., Sect. B: Struct. Sci.* **2002**, *58*, 380−388.
(17) Wilson, R. E.; Skanthakumar, S.; Sigmon, G.; Burns, P. C.; Soderholm, L. Structures of Dimeric Hydrolysis Products of Thorium. *Inorg. Chem.* **2007**, *46*, 2368−2372.
(18) Sokolov, M. N.; Gushchin, A. L.; Kovalenko, K. A.; Peresypkina, E. V.; Virovets, A. V.; Sanchiz, J.; Fedin, V. P. Triangular Oxalate Clusters $[W_3(\mu_3\text{-}S)(\mu_2\text{-}S_2)_3(C_2O_4)_3]^{2-}$ as Building Blocks for Coordination Polymers and Nanosized Complexes. *Inorg. Chem.* **2007**, *46*, 2115−2123.
(19) Pohl, R. W. H.; Wiebke, J.; Klein, A.; Dolg, M.; Maggiarosa, N. A New 5,5′-Bitetrazole Thorium(IV) Compound: Synthesis, Crystal Structure and Quantum Chemical Investigation. *Eur. J. Inorg. Chem.* **2009**, *2009*, 2472−2476.
(20) Johansson, G.; Tansuriwongs, P.; Fontell, K.; Larsen, C.; Pedersen, C.; Rosén, U. The Structure of a dinuclear hydroxo complex of thorium. *Acta Chem. Scand.* **1968**, *22*, 389−398.
(21) Bino, A.; Chayat, R. A new hydroxo-bridged thorium (IV) dimer: Preparation and structure of di-$\mu$-hydroxo-bis[aquanitrato(2,6-diacetylpyridinedisemicarbazone) thorium (IV)] nitrate tetrahydrate. *Inorg. Chim. Acta* **1987**, *129*, 273−276.
(22) Kadish, K. M.; Liu, Y. H.; Anderson, J. E.; Charpin, P.; Chevrier, G.; Lance, M.; Nierlich, M.; Vigner, D.; Dormond, A.; Belkalem, B.; Guilard, R. First example of a trimeric metalloporphyrin. Synthesis, electrochemical, and spectroelectrochemical studies of $[(P)Th(OH)_2]_3$ where P is the dianion of octaethyl- or tetraphenylporphyrin. Crystal structure of a dihydrated trinuclear complex of dihydroxy(5,10,15,20-tetraphenylporphinato)thorium(IV) heptane solvate. *J. Am. Chem. Soc.* **1988**, *110*, 6455−6462.
(23) Duval, S.; Béghin, S. b.; Falaise, C. m.; Trivelli, X.; Rabu, P.; Loiseau, T. Stabilization of Tetravalent 4f (Ce), 5d (Hf), or 5f (Th, U) Clusters by the $[\alpha\text{-}SiW_9O_{34}]^{10-}$ Polyoxometalate. *Inorg. Chem.* **2015**, *54*, 8271−8280.
(24) Martin, N. P.; Volkringer, C.; Falaise, C.; Henry, N.; Loiseau, T. Synthesis and Crystal Structure Characterization of Thorium Trimesate Coordination Polymers. *Cryst. Growth Des.* **2016**, *16*, 1667−1678.
(25) Li, Y.; Yang, Z.; Wang, Y.; Bai, Z.; Zheng, T.; Dai, X.; Liu, S.; Gui, D.; Liu, W.; Chen, M.; Chen, L.; Diwu, J.; Zhu, L.; Zhou, R.; Chai, Z.; Albrecht-Schmitt, T. E.; Wang, S. A mesoporous cationic thorium-organic framework that rapidly traps anionic persistent organic pollutants. *Nat. Commun.* **2017**, *8*, 1354.
(26) Rogers, R. D.; Bond, A. H.; Witt, M. M. Macrocycle complexation chemistry 34. Polyethylene glycol and glycolate complexes of $Th^{4+}$. Preparation and structural characterization of $[ThCl_3(\text{pentaethylene glycol})]Cl{\cdot}CH_3CN$ and the $(Th^{4+})_4$ cluster, $[Th_4Cl_8(O)(\text{tetraethylene glycolate})_3]{\cdot}3CH_3CN$. *Inorg. Chim. Acta* **1991**, *182*, 9−17.
(27) Lin, J.; Jin, G. B.; Soderholm, L. $Th_3[Th_6(OH)_4O_4(H_2O)_6]\text{-}(SO_4)_{12}(H_2O)_{13}$: A Self-Assembled Microporous Open-Framework Thorium Sulfate. *Inorg. Chem.* **2016**, *55*, 10098−10101.
(28) Knope, K. E.; Wilson, R. E.; Vasiliu, M.; Dixon, D. A.; Soderholm, L. Thorium(IV) Molecular Clusters with a Hexanuclear Th Core. *Inorg. Chem.* **2011**, *50*, 9696−9704.
(29) Vasiliu, M.; Knope, K. E.; Soderholm, L.; Dixon, D. A. Spectroscopic and Energetic Properties of Thorium(IV) Molecular Clusters with a Hexanuclear Core. *J. Phys. Chem. A* **2012**, *116*, 6917−6926.
(30) Hennig, C.; Takao, S.; Takao, K.; Weiss, S.; Kraus, W.; Emmerling, F.; Scheinost, A. C. Structure and stability range of a hexanuclear Th(IV)-glycine complex. *Dalton Trans.* **2012**, *41*, 12818−12823.
(31) Falaise, C.; Charles, J.-S.; Volkringer, C.; Loiseau, T. Thorium Terephthalates Coordination Polymers Synthesized in Solvothermal $DMF/H_2O$ System. *Inorg. Chem.* **2015**, *54*, 2235−2242.
(32) Vanagas, N. A.; Wacker, J. N.; Rom, C. L.; Glass, E. N.; Colliard, I.; Qiao, Y.; Bertke, J. A.; Van Keuren, E.; Schelter, E. J.; Nyman, M.; Knope, K. E. Solution and Solid State Structural Chemistry of Th(IV) and U(IV) 4-Hydroxybenzoates. *Inorg. Chem.* **2018**, *57*, 7259−7269.
(33) Takao, S.; Takao, K.; Kraus, W.; Emmerling, F.; Scheinost, A. C.; Bernhard, G.; Hennig, C. First Hexanuclear U-IV and Th-IV Formate Complexes - Structure and Stability Range in Aqueous Solution. *Eur. J. Inorg. Chem.* **2009**, *2009*, 4771−4775.
(34) Diwu, J.; Wang, S.; Albrecht-Schmitt, T. E. Periodic Trends in Hexanuclear Actinide Clusters. *Inorg. Chem.* **2012**, *51*, 4088−4093.
(35) Qian, X.-Y.; Zhou, T.-H.; Mao, J.-G. New thorium(IV)-arsonates with a $[Th_8O_{13}]^{6+}$ octanuclear core. *Dalton Trans.* **2015**, *44*, 13573−13580.
(36) Knope, K. E.; Vasiliu, M.; Dixon, D. A.; Soderholm, L. Thorium (IV)−selenate clusters containing an octanuclear Th (IV) hydroxide/oxide core. *Inorg. Chem.* **2012**, *51*, 4239−4249.
(37) Woidy, P.; Kraus, F. $[Th_{10}(\mu\text{-}F_{16})(\mu_3\text{-}O_4)(\mu_4\text{-}O_4)(NH_3)_{32}]\text{-}(NO_3)_8{\cdot}19.6\ NH_3$−the Largest Thorium Complex from Solution known to Date. *Z. Anorg. Allg. Chem.* **2014**, *640*, 1547−1550.
(38) Bruker. *APEX2, SADABS, SAINT, SHELXTL, XCIF, XPREP*; Bruker AXS, Inc.: Madison, WI, 2014.
(39) Ilavsky, J.; Jemian, P. R. Irena: tool suite for modeling and analysis of small angle scattering. *J. Appl. Crystallogr.* **2009**, *42*, 347−353.


DOI: 10.1021/acs.inorgchem.9b01238
*Inorg. Chem.* 2019, 58, 10871−10882

(40) Zhang, R.; Thiyagarajan, P.; Tiede, D. M. Probing protein fine structures by wide angle solution X-ray scattering. *J. Appl. Crystallogr.* **2000**, *33*, 565−568.
(41) Parr, R. G.; Yang, W. *Density-functional theory of atoms and molecules*; Oxford University Press: New York, 1989.
(42) Becke, A. D. Density-functional thermochemistry. III. The role of exact exchange. *J. Chem. Phys.* **1993**, *98*, 5648−5652.
(43) Lee, C.; Yang, W.; Parr, R. G. Development of the Colle-Salvetti correlation-energy formula into a functional of the electron density. *Phys. Rev. B: Condens. Matter Mater. Phys.* **1988**, *37*, 785.
(44) Godbout, N.; Salahub, D. R.; Andzelm, J.; Wimmer, E. Optimization of Gaussian-type basis sets for local spin density functional calculations. Part I. Boron through neon, optimization technique and validation. *Can. J. Chem.* **1992**, *70*, 560−571.
(45) Dunning, T. H., Jr. Gaussian basis sets for use in correlated molecular calculations. I. The atoms boron through neon and hydrogen. *J. Chem. Phys.* **1989**, *90*, 1007−1023.
(46) Kendall, R. A.; Dunning, T. H., Jr; Harrison, R. J. Electron affinities of the first-row atoms revisited. Systematic basis sets and wave functions. *J. Chem. Phys.* **1992**, *96*, 6796−6806.
(47) Woon, D. E.; Dunning, T. H., Jr Gaussian basis sets for use in correlated molecular calculations. III. The atoms aluminum through argon. *J. Chem. Phys.* **1993**, *98*, 1358−1371.
(48) Dunning, T. H., Jr; Peterson, K. A.; Wilson, A. K. Gaussian basis sets for use in correlated molecular calculations. X. The atoms aluminum through argon revisited. *J. Chem. Phys.* **2001**, *114*, 9244−9253.
(49) Peterson, K. A. Correlation consistent basis sets for actinides. I. The Th and U atoms. *J. Chem. Phys.* **2015**, *142*, No. 074105.
(50) Frisch, M.; Trucks, G.; Schlegel, H.; Scuseria, G.; Robb, M.; Cheeseman, J.; Scalmani, G.; Barone, V.; Mennucci, B.; Petersson, G. *Gaussian 09*; Gaussian, Inc. Wallingford, CT,2009, *6492*,.
(51) Møller, C.; Plesset, M. S. Note on an approximation treatment for many-electron systems. *Phys. Rev.* **1934**, *46*, 618.
(52) Pople, J. A.; Binkley, J. S.; Seeger, R. Theoretical models incorporating electron correlation. *Int. J. Quantum Chem.* **1976**, *10*, 1−19.
(53) Werner, H.-J.; Knowles, P. J.; Manby, F. R.; Schütz, M.; Celani, P.; Knizia, G.; Korona, T.; Lindh, R.; Mitrushenkov, A.; Rauhut, G.; et al.; *MOLPRO, version 2012.1, a package of ab initio programs, see* http://www.molpro.net.
(54) Tomasi, J.; Mennucci, B.; Cammi, R. Quantum mechanical continuum solvation models. *Chem. Rev.* **2005**, *105*, 2999−3094.
(55) Klamt, A. *COSMO-RS: from quantum chemistry to fluid phase thermodynamics and drug design*; Elsevier: 2005.
(56) Klamt, A.; Schüürmann, G. COSMO: a new approach to dielectric screening in solvents with explicit expressions for the screening energy and its gradient. *J. Chem. Soc., Perkin Trans. 2* **1993**, 799−805.
(57) Frisch, M. J.; Trucks, G. W.; Schlegel, H. B.; Scuseria, G. E.; Robb, M. A.; Cheeseman, J. R.; Montgomery, J.. J. A.; Vreven, T.; Kudin, K. N.; Burant, J. C.; et al. *Gaussian 03, Revision E.01*; Gaussian, Inc.: Wallingford, CT, 2004.
(58) Wilson, R. E.; Skanthakumar, S.; Burns, P. C.; Soderholm, L. Structure of the Homoleptic Thorium(IV) Aqua Ion $[Th(H_2O)_{10}]$-$Br_4$. *Angew. Chem., Int. Ed.* **2007**, *46*, 8043−8045.
(59) Minasian, S. G.; Boland, K. S.; Feller, R. K.; Gaunt, A. J.; Kozimor, S. A.; May, I.; Reilly, S. D.; Scott, B. L.; Shuh, D. K. Synthesis and Structure of $(Ph_4P)_2MCl_6$ (M = Ti, Zr, Hf, Th, U, Np, Pu). *Inorg. Chem.* **2012**, *51*, 5728−5736.
(60) Steiner, T. The Hydrogen Bond in the Solid State. *Angew. Chem., Int. Ed.* **2002**, *41*, 48−76.
(61) Jeffrey, G. A. *An Introduction to Hydrogen Bonding*; Oxford University Press: 1997.
(62) Spek, A. L. Structure validation in chemical crystallography. *Acta Crystallogr., Sect. D: Biol. Crystallogr.* **2009**, *65*, 148−155.
(63) Lin, J.; Qie, M.; Zhang, L.; Wang, X.; Lin, Y.; Liu, W.; Bao, H.; Wang, J. Probing the Influence of Acidity and Temperature to Th(IV) on Hydrolysis, Nucleation, and Structural Topology. *Inorg. Chem.* **2017**, *56*, 14198−14205.
(64) Miller, F. A. Spectra of X−H Systems (with Emphasis on O−H and N−H Groups). *Course Notes on the Interpretation of Infrared and Raman Spectra* **2004**, 163−178.
(65) Kang, D.; Dai, J.; Hou, Y.; Yuan, J. Structure and vibrational spectra of small water clusters from first principles simulations. *J. Chem. Phys.* **2010**, *133*, No. 014302.
(66) Carey, D. M.; Korenowski, G. M. Measurement of the Raman spectrum of liquid water. *J. Chem. Phys.* **1998**, *108*, 2669−2675.
(67) Cross, P. C.; Burnham, J.; Leighton, P. A. The Raman spectrum and the structure of water. *J. Am. Chem. Soc.* **1937**, *59*, 1134−1147.
(68) Otto, K. E.; Xue, Z.; Zielke, P.; Suhm, M. A. The Raman spectrum of isolated water clusters. *Phys. Chem. Chem. Phys.* **2014**, *16*, 9849−9858.
(69) Dolenko, T. A.; Burikov, S. A.; Dolenko, S. A.; Efitorov, A. O.; Plastinin, I. V.; Yuzhakov, V. I.; Patsaeva, S. V. Raman Spectroscopy of Water−Ethanol Solutions: The Estimation of Hydrogen Bonding Energy and the Appearance of Clathrate-like Structures in Solutions. *J. Phys. Chem. A* **2015**, *119*, 10806−10815.
(70) Katz, J.; Seaborg, G. *The Chemistry of the Actinide Elements*; Methuen: London, 1957; p *96*.
(71) Bagnall, K. The coordination chemistry of the actinide halides. *Coord. Chem. Rev.* **1967**, *2*, 145−162.
(72) Siegel, S. The structures of $Cs_2ThCl_6$ and $Cs_2UCl_6$. *Acta Crystallogr.* **1956**, *9*, 827−827.
(73) Bossé, E.; Den Auwer, C.; Berthon, C.; Guilbaud, P.; Grigoriev, M. S.; Nikitenko, S.; Naour, C. L.; Cannes, C.; Moisy, P. Solvation of $UCl_6^{2-}$ Anionic Complex by $MeBu_3N^+$, $BuMe_2Im^+$, and $BuMeIm^+$ Cations. *Inorg. Chem.* **2008**, *47*, 5746−5755.
(74) Nikitenko, S. I.; Hennig, C.; Grigoriev, M. S.; Naour, C. L.; Cannes, C.; Trubert, D.; Bossé, E.; Berthon, C.; Moisy, P. Structural and spectroscopic studies of the complex $[BuMeIm]_2[UCl_6]$ in the solid state and in hydrophobic room temperature ionic liquid $[BuMeIm][Tf_2N]$. *Polyhedron* **2007**, *26*, 3136−3142.
(75) Wilson, R. E. Structure, Phase Transitions, and Isotope Effects in $[(CH_3)_4N]_2PuCl_6$. *Inorg. Chem.* **2015**, *54*, 10208−10213.
(76) Wilson, R. E.; Schnaars, D. D.; Andrews, M. B.; Cahill, C. L. Supramolecular Interactions in $PuO_2Cl_4^{2-}$ and $PuCl_6^{2-}$ Complexes with Protonated Pyridines: Synthesis, Crystal Structures, and Raman Spectroscopy. *Inorg. Chem.* **2014**, *53*, 383−392.
(77) Ferraro, J. R. Some complex chlorides of uranium tetrachloride and thorium tetrachloride. *J. Inorg. Nucl. Chem.* **1957**, *4*, 283−286.
(78) Tsushima, S.; Yang, T. Relativistic density functional theory study on the structure and bonding of U(IV) and Np(IV) hydrates. *Chem. Phys. Lett.* **2005**, *401*, 68−71.
(79) Hennig, C.; Tutschku, J.; Rossberg, A.; Bernhard, G.; Scheinost, A. C. Comparative EXAFS investigation of uranium(VI) and -(IV) aquo chloro complexes in solution using a newly developed spectroelectrochemical cell. *Inorg. Chem.* **2005**, *44*, 6655−6661.
(80) Cantat, T.; Scott, B. L.; Kiplinger, J. L. Convenient access to the anhydrous thorium tetrachloride complexes $ThCl_4(DME)_2$, $ThCl_4(1,4\text{-dioxane})_2$ and ThCl4$(THF)_{3.5}$ using commercially available and inexpensive starting materials. *Chem. Commun.* **2010**, *46*, 919−921.
(81) Rogers, R. D.; Bond, A. H. Structure of $[ThCl(OH)(OH_2)_6]$-$2Cl_4\cdot$18-crown-6.$2H_2O$. *Acta Crystallogr., Sect. C: Cryst. Struct. Commun.* **1992**, *48*, 1199−1201.
(82) Spry, M.; Errington, W.; Willey, G. R. Aquatetrachlorotris (tetrahydrofuran-O) thorium (IV) Tetrahydrofuran Solvate (1/1). *Acta Crystallogr., Sect. C: Cryst. Struct. Commun.* **1997**, *53*, 1388−1390.
(83) Rogers, R. D. Macrocycle complexation chemistry. Pt. 31. *Lanthanide Actinide Res.* **1989**, *3*, 71−81.
(84) Surbella, R. G.; Ducati, L. C.; Pellegrini, K. L.; McNamara, B. K.; Autschbach, J.; Schwantes, J. M.; Cahill, C. L. A new Pu(III) coordination geometry in $(C_5H_5NBr)_2[PuCl_3(H_2O)_5]\cdot$2Cl·$2H_2O$ as obtained via supramolecular assembly in aqueous, high chloride media. *Chem. Commun.* **2017**, *53*, 10816−10819.


DOI: 10.1021/acs.inorgchem.9b01238
*Inorg. Chem.* 2019, 58, 10871−10882

(85) Wilson, R. E.; Almond, P. M.; Burns, P. C.; Soderholm, L. The Structure and Synthesis of Plutonium(III) Chlorides from Aqueous Solution. *Inorg. Chem.* **2006**, *45*, 8483−8485.
(86) Kraus, K. A.; Moore, G. E.; Nelson, F. Anion-exchange Studies. XXI. Th(IV) and U(IV) in hydrochloric acid. Separation of thorium, protactinium, and uranium[1,2]. *J. Am. Chem. Soc.* **1956**, *78*, 2692−2695.
(87) Ryan, J. L. Actinide(IV) Chloride Species Absorbed by Anion Exchange Resins from Chloride Solutions. *J. Phys. Chem.* **1961**, *65*, 1856−1859.
(88) Fuger, J.; Brown, D. Thermodynamics of the actinide elements. Part III. Heats of formation of the dicaesium actinide hexachloro-complexes. *J. Chem. Soc. A* **1971**, 841−846.
(89) Clark, D. L.; Grumbine, S. K.; Scott, B. L.; Watkin, J. G. Sterically Demanding Aryloxides as Supporting Ligands in Organo-actinide Chemistry. Synthesis, Structural Characterization, and Reactivity of $Th(O\text{-}2,6\text{-}t\text{-}Bu_2C_6H_3)_2(CH_2SiMe_3)_2$ and Formation of the Trimeric Thorium Hydride $Th_3H_6(O\text{-}2,6\text{-}t\text{-}Bu_2C_6H_3)_6$. *Organo-metallics* **1996**, *15*, 949−957.
(90) Ok, K. M.; Sung, J.; Hu, G.; Jacobs, R. M. J.; O'Hare, D. TOF-2: A Large 1D Channel Thorium Organic Framework. *J. Am. Chem. Soc.* **2008**, *130*, 3762−3763.
(91) Galley, S. S.; Van Alstine, C. E.; Maron, L.; Albrecht-Schmitt, T. E. Understanding the Scarcity of Thorium Peroxide Clusters. *Inorg. Chem.* **2017**, *56*, 12692−12694.
(92) Ekberg, C.; Albinsson, Y.; Comarmond, M. J.; Brown, P. L. Studies on the complexation behavior of thorium (IV). 1. Hydrolysis equilibria. *J. Solution Chem.* **2000**, *29*, 63−86.
(93) Neck, V.; Kim, J. Solubility and hydrolysis of tetravalent actinides. *Radiochim. Acta* **2001**, *89*, 1−16.
(94) Knope, K. E.; Wilson, R. E.; Skanthakumar, S.; Soderholm, L. Synthesis and Characterization of Thorium(IV) Sulfates. *Inorg. Chem.* **2011**, *50*, 8621−8629.
(95) Knope, K. E.; Wilson, R. E.; Vasiliu, M.; Dixon, D. A.; Soderholm, L. Thorium (IV) molecular clusters with a hexanuclear Th core. *Inorg. Chem.* **2011**, *50*, 9696−9704.
(96) Torapava, N.; Persson, I.; Eriksson, L.; Lundberg, D. Hydration and hydrolysis of thorium (IV) in aqueous solution and the structures of two crystalline thorium (IV) hydrates. *Inorg. Chem.* **2009**, *48*, 11712−11723.



DOI: 10.1021/acs.inorgchem.9b01238
*Inorg. Chem.* 2019, 58, 10871−10882